Adv. Polar Upper Atmos. Res., **15**, 32-42, 2001

Seasonal dependence of the vertical distributions of auroral kilometric radiation sources and auroral particle acceleration regions observed by the Akebono satellite

Atsushi Kumamoto[1], Takayuki Ono[1] and Hiroshi Oya[2]

[1] *Department of Geophysics, Graduate School of Science, Tohoku University, Aoba, Aramaki, Aoba-ku, Sendai 980-8578*

[2] *Fukui University of Technology, Gakuen 3-6-1, Fukui 910-8505*

Abstract: Seasonal variations in the vertical distributions of occurrence probabilities of auroral kilometric radiation (AKR) sources and auroral acceleration regions indicated by upward-flowing ion (UFI) events were compared based on statistical analyses of plasma waves and energetic particles data observed by the Akebono satellite. The peak altitude in the vertical distribution of occurrence probability of AKR sources whose emission intensities were larger than $-150\,\mathrm{dBW/m^2 \cdot Hz}$ occurred at 5000-6000 km in the summer polar region and at 3000-4000 km in the winter polar region. The analyses have also clarified that the vertical distributions of occurrence probabilities of auroral acceleration regions also show seasonal variations that are quite similar to those of the AKR sources. Based on the observation that intense AKR emissions can be generated even in high-density plasma, we suggest that processes other than cyclotron maser instability (CMI), such as mode conversions, may be dominant under conditions of dense ambient plasma in the summer polar regions. The contribution of the emissions generated by these mechanisms to the seasonal variations in the vertical distributions of AKR sources is thought to be significant.

1. Introduction

In recent studies of auroral phenomena, seasonal variations in auroral kilometric radiation (AKR) sources and precipitating auroral particles have been found through statistical analyses of observation data. The analysis of auroral particle data collected by the DMSP satellite over a nine-year period has revealed a seasonal dependence; that is, the occurrence probabilities of accelerated auroral electrons are suppressed during summer or in the presence of sunlight (Newell *et al.*, 1996). A seasonal variation in AKR has also been identified in the distant magnetotail using data obtained by the GEOTAIL spacecraft (Kasaba *et al.*, 1997) and the Akebono satellite in a near-earth polar orbit (Kumamoto and Oya, 1998). Kasaba *et al.* (1997) have shown that the AKR occurrence probabilities, as observed by the GEOTAIL spacecraft at a distance of more than 10 R_E in the ecliptic plane, were asymmetric in the summer and winter hemispheres. They concluded that AKR is more active in the winter hemisphere. Kumamoto and Oya (1998) provided a more complete and extensive confirmation of this seasonal asymmetry in occurrence probabilities and AKR intensity based on the data obtained by the plasma wave observation and sounder experiments (PWS) system

on board the Akebono satellite over a 7-year period. From the Akebono satellite, which is on a polar orbit within a geocentric distance of $2.6R_E$, AKR observations can be carried out for all latitude ranges of sources in both hemispheres without the shading effects of the plasmasphere and ambiguities rising from propagations. Furthermore, seasonal dependences of auroral EMIC waves (Erlandson and Zanetti, 1998) and UV from aurora (Liou *et al.*, 1997) have also been reported in recent studies.

Interactions between energetic electrons and magnetoactive plasma in the auroral plasma cavity are thought to be an important factor controlling the generation of AKR. These interactions have been mainly investigated using the theory of cyclotron maser instability (CMI) (Wu and Lee, 1979; Dusenbery and Lyons, 1982; Omidi *et al.*, 1984; Menietti *et al.*, 1993; Roux *et al.*, 1993). As a control mechanism for the seasonal variation in auroral electrons, the conductivity of the ionosphere is thought to change the resonance conditions of the field-aligned AC currents (Newell *et al.*, 1996). For the seasonal variations in AKR, Kasaba *et al.* (1997) proposed that up-welling plasma from the summer ionosphere hinders or violates the generation conditions required for CMI processes.

To investigate the relation between the distribution of AKR sources and the auroral particle acceleration regions, it is useful to analyze the upward flowing ions (UFI). When the acceleration regions are formed below the satellite, they do not only accelerate the electrons downward, but they also move the ions upward. We used these UFI events to indicate the existence of an acceleration region below the satellite (Shelley *et al.*, 1976; Ghielmetti *et al.*, 1978).

In this paper, we analyzed long-term observations of AKR and UFI phenomena obtained by the Akebono satellite to investigate the processes that control AKR activities based on the relationship between the vertical distributions of the AKR sources and the auroral acceleration regions.

2. Seasonal dependence of vertical distributions of AKR sources

In the present study, plasma wave data observed by the PWS system on board the Akebono satellite between March 1989 and August 1999 (including at least 13753 hours of observation in the northern hemisphere and 10575 hours in the southern hemisphere) were used to analyze AKR. The instrumentation of the PWS system has been precisely described by Oya *et al.* (1990). For the statistical analysis, the coverage region of the Akebono satellite's orbit below an altitude level of 7000 km in geomagnetic latitude ranges of higher than 45° was divided into 14 altitudinal bins; the vertical size of each of these bins was 500 km. An upper altitude limit of 7000 km was determined by the apogee of the Akebono satellite in 1999. The probability that an AKR source would occur was then calculated for each altitudinal bin. An AKR occurrence was defined as an emission intensity larger than $-150\,\mathrm{dBW/m^2 \cdot Hz}$. The altitudes of the AKR sources were determined by assuming that the AKR emission frequency was nearly equal to the electron cyclotron frequency at the source points. Though the actual emission frequency is slightly larger than the electron cyclotron frequency, the vertical resolution of the analysis was confined to an altitude of within 500 km, even for cases where the AKR emission frequency was 10% larger than the electron cyclotron

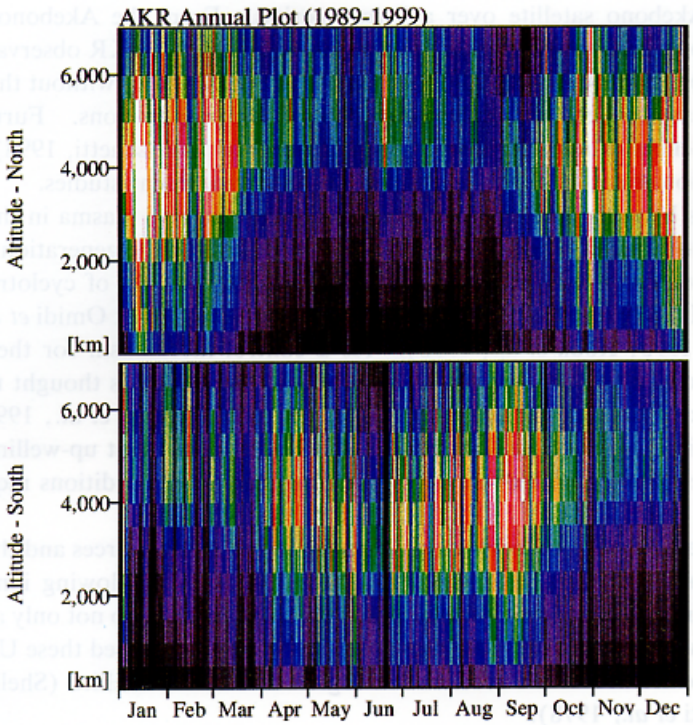

Fig. 1. Seasonal variations in the vertical distributions of occurrence probabilities of AKR sources whose emission intensities are larger than $-150\,dBW/m^2 \cdot Hz$. The upper and lower panels are based on observations in the northern and southern polar regions, respectively. Each plot shows the month versus the altitude.

frequency at the source points.

Figure 1 shows the results of the analysis on the occurrence probabilities of AKR sources; the horizontal axis indicates the months from January to December, and the vertical axis indicates the source altitude of the AKR. The upper panel in Fig. 1 represents the observations in the northern polar region, and the lower panel represents the southern polar region. The figure clearly shows that the peak altitude in the vertical distribution of AKR source occurrence probabilities is at 5000–6000 km in the summer polar region and 3000–4000 km in the winter polar region. The values of the occurrence probability peaks are within 1%, even for the maximum case.

3. Seasonal dependence of vertical distributions of UFI events

Previous analyses have clarified that the peak altitude in the vertical distribution of AKR source occurrence probabilities varies, depending on the season. To investigate the relationship of this finding with the vertical distribution of the auroral particle acceleration regions, we analyzed the occurrence probabilities of UFI events in terms of the vertical distribution. In a study on long-term variations in UFI events, Yau *et al.* (1985) identified seasonal variations in the occurrence frequency of UFI events using

observations from the DE-1 satellite at a high altitude of between 8000 km and 23300 km.

In the present study, we used UFI events to indicate the presence of auroral acceleration regions. Since UFI events occur over all auroral acceleration regions along the magnetic fields, the occurrence probability of a UFI event should equal the sum of the occurrence probabilities for all auroral acceleration regions below the satellite. Thus the vertical distribution of the occurrence probability of an auroral acceleration region can be derived from the vertical distribution of UFI events. Ener-

Table 1. Fifteen bins used to calculate the average number fluxes of energetic ions observed by the LEP system on board the Akebono satellite.

	0–30° (Upward)	30–60° (Perpendicular)	60–90° (Downward)
34.6–124 eV	U1	P1	D1
124–343 eV	U2	P2	D2
343 eV–1.22 keV	U3	P3	D3
1.22–3.39 keV	U4	P4	D4
3.39–12.1 keV	U5	P5	D5

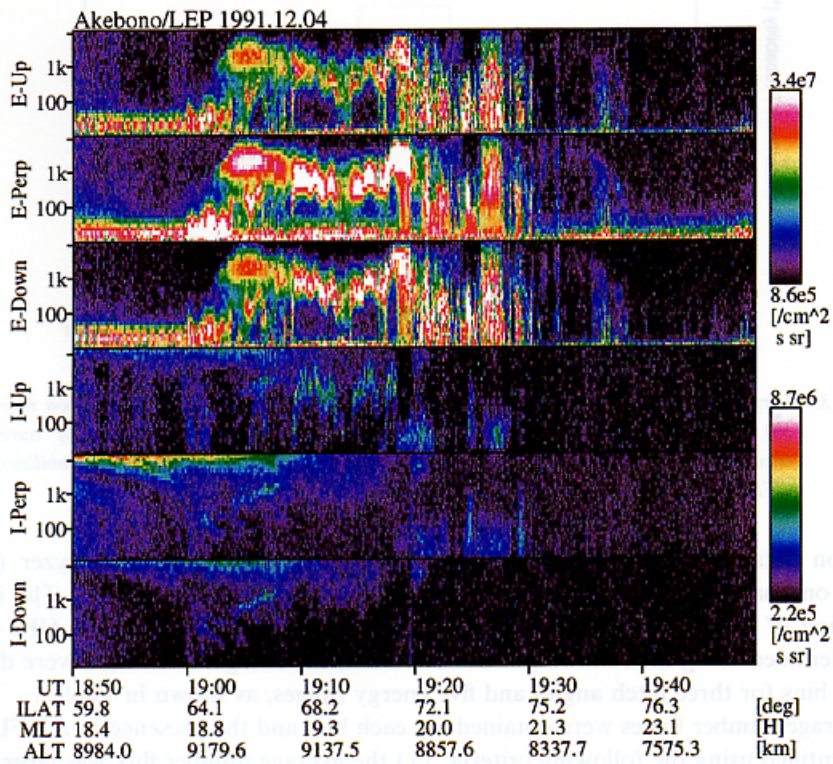

Fig. 2. Example of UFI events. In this observation, performed on December 4, 1991, UFI events are seen from 1910 UT to 1920 UT.

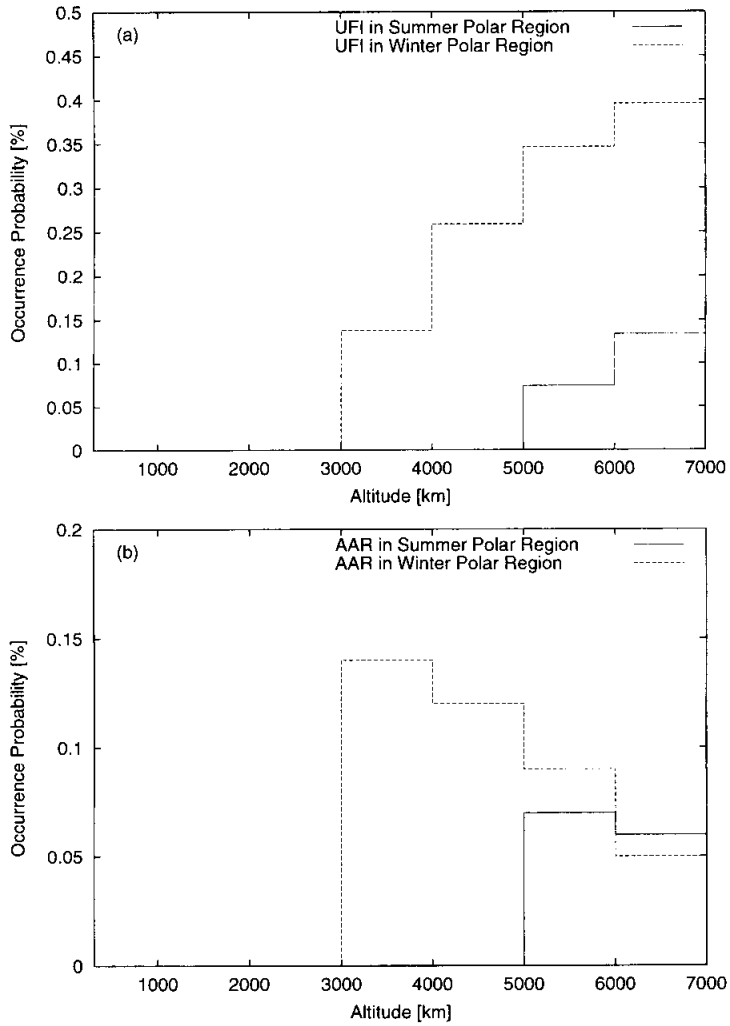

Fig. 3. Vertical distributions of occurrence probabilities of UFI events (a) and acceleration regions (b) in the summer and winter polar regions. Occurrence probabilities of auroral acceleration regions are derived from the differences between the occurrence probabilities of UFI events in two neighboring altitude ranges.

getic ion data observed by the low-energy charged particle spectra analyzer (LEP) system on board the Akebono satellite were used to analyze UFI events. The instrumentation of the LEP system has been described by Mukai *et al.* (1990). UFI events were identified using the following method. First, the energetic ion data were divided into 15 bins for three pitch angles and five energy ranges, as shown in Table 1. Then, the average number fluxes were obtained for each bin, and the presence of a UFI event was identified using the following criteria; (1) the average number flux was larger than 1.4×10^6 eV/(cm^2·s·sr·eV), (2) the average number flux in upward ions with an energy range larger than 343 eV was larger than 1.7 times the average number flux of upward

ions with a lower energy range, and (3) the average number flux in upward ions with an energy range larger than 343 eV was larger than 1.7 times the average number flux of perpendicular and downward ions. An example of an identified UFI event is displayed in Fig. 2.

Using the present method for identifying UFI events, the seasonal variation in the altitude of UFI events was investigated for the period from April 1989 to January 1997. The vertical distributions of UFI event occurrence probabilities in the summer and winter polar regions are shown in Fig. 3a. Furthermore, the vertical distributions of the auroral acceleration regions derived from the difference between the occurrence probabilities of UFI events in the two neighboring altitude ranges are indicated in Fig. 3b. The figures show that the peak altitude in the vertical distribution of auroral acceleration region occurrence probabilities varies according to the season with the same tendency as the variation of AKR sources. This finding suggests a close correlation between the vertical distributions of AKR sources and auroral acceleration regions. The values of the occurrence probability peaks for the auroral acceleration regions are 0.14% and 0.07% for the summer and winter polar regions, respectively. These values are similar to those for the AKR sources.

4. AKR sources in high density plasma regions

The up-welling plasma hypothesis proposed by Kasaba *et al.* (1997) explains the seasonal variations in AKR by the change in ambient plasma density at their sources. The hypothesis is based on the CMI theory, which is strictly controlled by the plasma density; in other words, the CMI process only works in tenuous plasma (Wu and Lee, 1979). The association between plasma density depletions and AKR sources has been documented by a number of observational studies (Benson and Calvert, 1979; Benson *et al.*, 1980; Calvert, 1981; Persoon *et al.*, 1988; Strangeway *et al.*, 1998). However, the data obtained by the Akebono satellite show that AKR sources can be observed even in regions of high-density plasma.

An example of an AKR source in a high-density plasma region is shown in Fig. 4. The top panel shows the dynamic spectra of AKR, with solid and dotted curves indicating the local electron cyclotron frequency (f_c) and the local R-X mode cutoff frequency (f_x), respectively. The solid line corresponds to 181 kHz, which is the observation frequency of the Poyinting flux measurements that are also performed by the PWS system. In the second panel, the plasma parameters f_p/f_c are indicated, where the plasma frequency (f_p) is derived from the upper limit frequency of UHR and whistler waves. The actual upper limit frequencies of the whistler waves may be lower than f_p, depending on the propagation angles with respect to the magnetic field. However, even using underestimated f_p/f_c ratios, sufficient evidence was obtained to confirm that high-density plasma regions exist. The third panel shows the axial ratios of emissions with a frequency of 181 kHz determined by the Poyinting flux measurements. The axial ratios were defined as positive for right-handed waves and negative for left-handed waves with respect to the magnetic field. In bottom two panels, the distances between the satellite and the sources of right-handed and left-handed AKR are indicated, based on the use of the Poynting flux measurements to determine the location

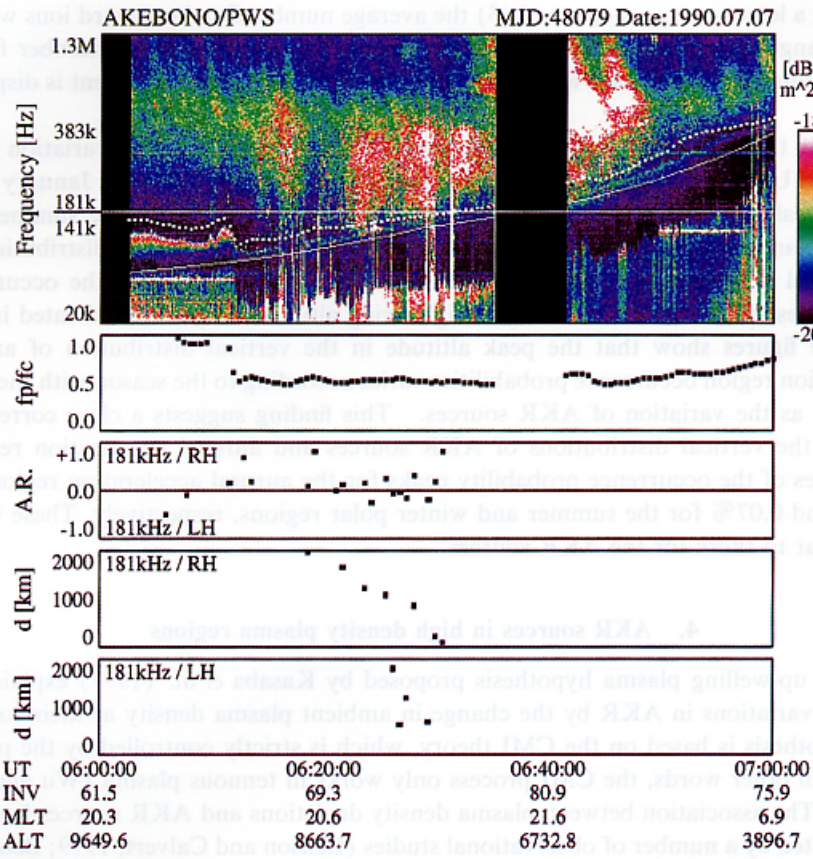

Fig. 4. Example of AKR emissions generated in high f_p/f_c plasma, observed on July 7, 1990. In the upper panel, the dynamic spectra are shown with solid and dotted curves indicating f_c and f_x, respectively. The solid line represents 181 kHz, the observation frequency of the Poyinting flux measurements. In the second panel, the f_p/f_c ratios at the satellite positions are plotted. The third panel shows the axial ratios of emissions with a frequency of 181 kHz determined by the Poyinting flux measurements. Axial ratios are defined as positive for right-handed waves and negative for left-handed waves. The distances between the satellite and the identified sources of right-handed and left-handed AKR with a frequency of 181 kHz are given in bottom two panels.

of the AKR sources. This calculation is performed by measuring the wave form of the three components of the AKR's magnetic field and deriving the directions of the AKR's k-vector using the Means method (Means, 1972). The locations of the sources are then determined using the k-vector directions and the AKR emission frequencies, assuming that the path of the radiation is approximately straight and that the emission frequency is nearly equal to the electron cyclotron frequency at the source point.

In the case shown in Fig. 4, the satellite entered the AKR source region at around 0622 UT. Observing the mixed emissions of R-X and L-O mode AKR, shown by the axial ratios, the satellite can be shown to have encountered the source of the R-X mode AKR with a frequency of 181 kHz around 0630 UT, which is also suggested by the

electrostatic waves that can accompany the electron beams and the small gap between the AKR emission frequency and the local R-X mode cutoff frequency (f_x). The ratios of f_p/f_c are always larger than 0.5 around the source encounter. CMI processes can not generate R-X mode emissions when $f_p/f_c > 0.3$. Therefore, the AKR emissions in Fig. 4 are probably generated by other mechanisms, such as mode conversions. The CMI mechanism and mode conversion mechanism are considered to co-exist in AKR sources. However, in high-density plasma regions, emissions originating from the CMI mechanism disappear, and emissions originating from mode conversion mechanisms are thought to become dominant. These emissions may contribute to the vertical distributions of AKR sources indicated in Section 2, especially at low altitudes where the ambient plasma density is relatively high.

5. Discussion

The main results of our analyses are summarized bellow:

1) The vertical distributions of AKR sources, which are derived from the AKR emission frequencies, show distinct seasonal variations; the peak altitude in the vertical distribution of AKR source occurrence probability occurs at 5000–6000 km in the summer polar region and 3000–4000 km in the winter polar region.

2) The vertical distributions of the auroral particle acceleration regions were described, based on the analyses of the occurrence probabilities of UFI events observed by the Akebono satellite. The results show that the peak altitude in the vertical distribution of auroral acceleration region occurrence probability occurs at 5000–6000 km in the summer polar region, and drops to 3000–4000 km in the winter polar region. The similarity in the seasonal variations of AKR sources and auroral acceleration regions suggests a close correlation.

3) AKR sources in high-density plasma regions, where the ratio of f_p/f_c was larger than 0.5, were identified in the plasma wave data observed by the Akebono satellite. These regions suggest the possibility that mechanisms other than CMI become dominant during generation of AKR in high plasma density region.

The results show that AKR sources and auroral particle acceleration regions have similar vertical distributions that depend on the season. Based on CMI theory, the anisotropy of upward electrons in a loss-cone distribution contribute to the generation of intense R-X mode emissions. Downward accelerations of electrons by field-aligned electric field, indicated by UFI events, cause large losses at magnetic mirror points located at altitude near the top of the ionosphere and exhibit a loss-cone distribution with effective anisotropy for the generation of CMI emissions in the altitude range of AKR sources. However, because the anisotropy of upward electrons changes gradually in the vertical direction, the vertical distributions of CMI-mechanism AKR sources are thought to depend mainly on the density of the ambient plasma, rather than the vertical distribution of the acceleration regions.

The analyses of AKR sources in high-density plasma regions suggest that generation mechanisms other than CMI, such as mode conversions, are dominant under high-density plasma conditions. In mode conversion processes, irregularities in potential structures are expected to be source regions of intense UHR waves, since localized

electron beams corresponding to each potential structure generate UHR waves *via* inverse Landau resonance. Then, UHR waves are converted into R-X mode AKR *via* the Doppler mode conversion process, in which the frequencies of UHR waves are shifted upwards by the Doppler effect between ambient plasma and downwards moving plasma in auroral regions (Oya, 1990). Based on numerical calculations (Kumamoto, 2000), the growth rates of inverse Landau resonance increase as the ambient plasma density increases; the energy conversion rates of Doppler mode conversion processes are larger than 70 %, even in dense ambient plasma where the f_p/f_c ratio is 0.7. Therefore, AKR sources generated by mode conversion processes are not controlled by the ambient plasma density, but accompany the acceleration regions of auroral electrons.

The most plausible control factors for the seasonal variations of the acceleration regions are ambient plasma density and temperature. The seasonal control factors for the potential mechanisms of acceleration regions have been inferred as follows: For the mechanism of anomalous resistivity by electrostatic ion cyclotron waves, the effective collision rate was found to depend on the ambient plasma temperature (Hudson *et al.*, 1978). Low temperatures, expected in the winter polar region, are conducive to high effective collision rates, or large field-aligned potentials. In the mechanism for weak double layers, the potential (ϕ) and spatial size (L) of each double layer are proportional to the temperature and Debye length, respectively (Bernes *et al.*, 1985). Therefore, because the lifetime τ is determined by $\tau \sim L/\sqrt{e\phi/m} \propto 1/\sqrt{N}$ (Tetreault, 1991), the time-averaged potentials are expected to be large in the winter polar region due to the reduction in ambient plasma density (N). For the mechanism of inertial Alfven waves, feedback instability mechanisms are thought to control the amplitude of Alfven waves, as pointed out by Newell *et al.* (1996). Based on Lysak (1991), the growth rates of feedback instability become small when the ratio of Pedersen conductivity to ionospheric Alfven admittance, which is proportional to the square root of ambient plasma density ($\sqrt{N}$), is large in the summer polar region. For all mechanisms, the total potential of the acceleration regions is thought to be large in the winter polar regions and small in the summer polar regions.

The interpretation that seasonal variations in AKR sources are not directly controlled by ambient plasma density but simply accompany auroral particle acceleration regions should be examined by evaluating seasonal variations in occurrence frequency and the intensity of AKR and auroral particle acceleration regions, based on observations of plasma density and temperature. Long-term variations in plasma density and temperature in the polar regions above the ionosphere have not yet been fully clarified. Therefore, the next stage of this research will investigate the behavior of seasonal variations in ambient plasma density in the polar regions by the statistical analysis of the frequencies of UHR and whistler waves in order to describe the relations between AKR activities and ambient plasma parameters in greater detail.

Acknowledgments

We would like to thank the staff of the Akebono satellite team. The data of energetic ions observed by the LEP system on board the Akebono satellite were provided by the Akebono Science Data Base (SDB).

The editor thanks Drs. H. Yamagishi and P. Newell for their help in evaluating this paper.

References

Barnes, C., Hudson, M.K. and Lotko, W. (1985): Weak double layers in ion acoustic turbulence. Phys. Fluids, **28**, 1055–1062.

Benson, R.F. and Calvert, W. (1979): ISIS-1 observations at the source of auroral kilometric radiation. Geophys. Res. Lett., **6**, 479–482.

Benson, R.F., Calvert, W. and Klumpar, D.M. (1980): Simultaneous wave and particle observations in the auroral kilometric radiation source region. Geophys. Res. Lett., **7**, 959–962.

Calvert, W. (1981): The auroral plasma cavity. Geophys. Res. Lett., **8**, 919–921.

Dusenbery, P.B. and Lyons, L.R. (1982): General concepts on the generation of auroral kilometric radiation. J. Geophys. Res., **87**, 7467–7481.

Erlandson, R.E. and Zanetti, L.J. (1998): A statistical study of auroral electromagnetic ion cyclotron waves. J. Geophys. Res., **103**, 4627–4636.

Ghielmetti, A.G., Johnson, R.G., Sharp, R.D. and Shelley, E.G. (1978): The latitudinal, diurnal, and attitudinal distributions of upward flowing energetic ions of ionospheric origin. Geophys. Res. Lett., **5**, 59–62.

Hudson, M.K., Lysak, R.L. and Mozer, F.S. (1978): Magnetic field-aligned potential drops due to electrostatic ion cyclotron turbulence. Geophys. Res. Lett., **5**, 143–146.

Kasaba, Y., Matsumoto, H., Hashimoto, K. and Anderson, R.R. (1997): The angular distribution of auroral kilometric radiation observed by the GEOTAIL spacecraft. Geophys. Res. Lett., **24**, 2483–2486.

Kumamoto, A. (2000): A study on the source of auroral kilometric radiation based on the observations by the Akebono (EXOS-D) satellite. Ph. D. thesis, Tohoku Univ.

Kumamoto, A. and Oya, H. (1998): Asymmetry of occurrence-frequency and intensity of AKR between summer polar region and winter polar region sources. Geophys. Res. Lett., **25**, 2369–2372.

Liou, K., Newell, P.T. and Meng, C.-I. (1997): Synoptic auroral distribution: A survey using Polar ultraviolet imagery. J. Geophys. Res., **102**, 27197–27205.

Lysak, R.L. (1991): Feedback instability of the ionospheric resonant cavity. J. Geophys. Res., **96**, 1553–1568.

Means, J.D. (1972): Use of the three-dimensional covariance matrix in analyzing the polarization properties of plasma waves. J. Geophys. Res., **77**, 5551–5559.

Menietti, J.D., Burch, J.L., Winglee, R.M. and Gurnett, D.A. (1993): DE-1 particle and wave observations in AKR source region regions. J. Geophys. Res., **98**, 5865–5879.

Mukai, T., Hirahara, M., Kaya, N., Sagawa, E. and Miyake, W. (1990): Low energy charged particle observations in the 'auroral' magnetosphere - First results from the Akebono (EXOS-D) satellite. J. Geomagn. Geoelectr., **42**, 479–496.

Newell, P.T., Meng, C.-I. and Lyons, K.M. (1996): Suppression of discrete aurorae by sunlight. Nature, **381**, 766–767.

Omidi, N., Wu, C.S. and Gurnett, D.A. (1984): Generation of auroral kilometric and Z mode radiation by the cyclotron maser mechanism. J. Geophys., **89**, 883–895.

Oya, H., Morioka, A., Kobayashi, K., Iizima, M., Ono, T., Miyaoka, H., Okada, T. and Obara, T. (1990): Plasma wave observation and sounder experiments (PWS) using the Akebono (EXOS-D) satellite-instrumentation and initial results including discovery of the high altitude equatorial plasma turbulence. J. Geomagn. Geoelectr., **42**, 411–442.

Oya, H. (1990): Origin of auroral kilometric radiation as conversion of the upper hybrid mode plasma waves. Proc. Jpn. Acad., **66**, Ser. B, 129–134.

Persoon, A.M., Gurnett, D.A., Peterson, W.K., Waite, J.H., Burch, J.L. and Green, J.L. (1988): Electron density depletions in the nightside auroral oval. J. Geophys. Res., **93**, 1871–1895.

Roux, A., Hilgers, H., De Feraudy, H., Le Queau, H.D., Louarn, P., Perraut, S., Bahnsen, A., Jespersen, M., Ungstrup, E. and Andre, M. (1993): Auroral kilometric radiation sources: *In situ* and remote observations from Viking. J. Geophys. Res., **98**, 11657–11670.

Shelley, E.G., Sharp, R.D. and Johnson, R.G. (1976): Satellite observations of an ionospheric acceleration mechanism. Geophys. Res. Lett., **3**, 654 656.

Strangeway, R.J., Kepko, L., Elphic, R.C., Carlson, C.W., Ergun, R.E., McFadden, J.P., Peria, W.J., Delory, G.T., Chaston, C.C., Temerin, M., Cattell, C.A., Mobius, E., Kistler, L.M., Klumpar, D.M., Peterson, W.K., Shelley, E.G. and Pfaff, R.F. (1998): FAST observations of VLF waves in the auroral zone. Geophys. Res. Lett., **25**, 2065–2068.

Tetreault, D. (1991): Theory of electric fields in the auroral acceleration region. J. Geophys. Res., **96**, 3549–3563.

Yau, A.W., Beckwith, P.H., Peterson, W.K. and Shelley, E.G. (1985): Long-term (solar cycle) and seasonal variations of upflowing ionospheric ion events at DE 1 altitudes. J. Geophys. Res., **90**, 6395 6407.

Wu, C.S. and Lee, L.C. (1979): A theory of the terrestrial kilometric radiation. Astrophys. J., **230**, 621–626.

(Received December 5, 2000; Revised manuscript accepted June 15, 2001)